could be used to generate flowfield density profile. Note that in Fig. 4 the reference hologram was made with model out, tunnel off, and the scene hologram was made with model in and tunnel on.

During this test series, runs were also made to determine if an interferogram could be made that reflected only the change in flowfield due to gas injection. This would facilitate both qualitative and quantitative determination of the effects of surface blowing. For these tests, the reference hologram was made with tunnel on, model in, but no surface blowing. Figure 5 shows infinite and finite interferograms of this case and clearly demonstrates that the effect of the mean flowfield, common to both cases, can be completely negated.

The asymmetry on the upper nose corner was traced to a slight leak in the porous material joint at this location. The effect of this leak on the asymmetry of the shock can be seen in Fig. 5b (upper right). It is seen that this test series demonstrates both system insensitivity to vibration and wide versatility in realistic applications.

Conclusions

Advances in technique and several new applications have been enumerated. These advances are seen as part of a continuing program to develop an automated production-type holographic interferometry system capable of three-dimensional quantitative flow-field measurement. Future work will be directed toward completion of the computerized reader scanner system described in Ref. 1.

Acknowledgment

This work was supported by the Naval Air Systems Command (AIR-310) under AIRTASK A310-3100/0041.

References

[1] Hannah, B. W. and Havener, A. G., "Applications of Automated Holographic Interferometry," presented at *International Congress on Instrumentation in Aerospace Simulation Facilities,* Ottawa, Canada, Sept. 1975, pp. 237-246.

[2] Havener, A. G. and Radley, R. J., "Supersonic Wind Tunnel Investigation Using Pulsed Laser Holography," Rept. 73-0148, Oct 1973.

[3] Radley, R. J. Jr., and Havener, A. G., "The Application of Dual Hologram Interferometry to Wind Tunnel Testing," *AIAA Journal,* Vol. 11, Sept. 1973, pp. 1332-1333.

Prediction of Turbulent Boundary Layers on Cones at Incidence

Kalle Kaups* and Tuncer Cebeci†
Douglas Aircraft Company, Long Beach, Calif.

Introduction

IN this Note, we discuss the prediction of turbulent boundary layers on circular cones at incidence by an efficient numerical method. The method employs the eddy-viscosity concept to model the Reynolds shear stress terms and has been previously used to compute two-dimensional boundary layers[1] and recently three-dimensional boundary layers.[2-4] Our method differs from the others[5,6] in that it utilizes a recent suggestion of Bradshaw et al.[7]; rather than using the $y/\sqrt{x}$-similarity variable to reduce the governing equations to a similarity form as is done for laminar flows, we use the y/x-similarity variable for turbulent flows. Our study shows that this scaling provides better agreement with experiment than the "old" procedure.

Received Sept. 16, 1976; revision received Feb. 7, 1977.

Index categories: Boundary Layers and Convective Heat Transfer—Turbulent.

*Senior Engineer/Scientist. Member AIAA.

†Chief Aerodynamics Engineer, Research. Member AIAA.

Governing Equations

The governing boundary-layer equations for compressible laminar and turbulent flows on a conical surface are given by the following equations:

Continuity:

$$\frac{\partial}{\partial x}(x\rho u)+\frac{\partial}{\partial \theta}(\rho w)+\frac{\partial}{\partial y}(x\overline{\rho v})=0 \tag{1}$$

x-Momentum:

$$\rho u\frac{\partial u}{\partial x}+\rho\frac{w}{x}\frac{\partial u}{\partial \theta}+\overline{\rho v}\frac{\partial u}{\partial y}-\rho\frac{w^2}{x}=\frac{\partial}{\partial y}\left(\mu\frac{\partial u}{\partial y}-\rho\overline{u'v'}\right) \tag{2}$$

θ-Momentum

$$\rho u\frac{\partial w}{\partial x}+\rho\frac{w}{x}\frac{\partial w}{\partial \theta}+\overline{\rho v}\frac{\partial w}{\partial y}+\rho\frac{uw}{x}=-\frac{1}{x}\frac{\mathrm{d}p}{\mathrm{d}\theta}$$

$$+\frac{\partial}{\partial y}\left(\mu\frac{\partial w}{\partial y}-\rho\overline{w'v'}\right) \tag{3}$$

Energy

$$\rho u\frac{\partial H}{\partial x}+\rho\frac{w}{x}\frac{\partial H}{\partial \theta}+\overline{\rho v}\frac{\partial H}{\partial y}=\frac{\partial}{\partial y}\left[\frac{\mu}{Pr}\frac{\partial H}{\partial y}\right.$$

$$\left.+\mu\left(1-\frac{1}{Pr}\right)\frac{\partial}{\partial y}\left(\frac{u^2+w^2}{2}\right)-\rho\overline{v'H'}\right] \tag{4}$$

Here $\overline{\rho v}=\rho v+\overline{\rho' v'}$; θ denotes the polar coordinate in the developed plane; x the coordinate along the generators; and y the coordinate normal to the surface; with w, u, v the velocities in the θ, x, and y directions.

At the windward stagnation line, $\theta=0$, the cross-flow momentum equation is singular since $w\equiv 0$. Taking into account the symmetry conditions and differentiating Eq. (3) with respect to θ, we can write it as

$$\rho u\frac{\partial w_\theta}{\partial x}+\rho\frac{w_\theta^2}{x}+\overline{\rho v}\frac{\partial w_\theta}{\partial y}+\rho\frac{uw_\theta}{x}=-\frac{1}{x}\frac{\mathrm{d}^2p}{\mathrm{d}\theta^2}$$

$$+\frac{\partial}{\partial y}\left[\mu\frac{\partial w_\theta}{\partial y}-\rho(\overline{w'v'})_\theta\right] \tag{5}$$

Noting that $w=0$, Eqs. (1, 2, and 4) can be simplified and written as

$$\frac{\partial}{\partial x}(x\rho u)+\rho w_\theta+\frac{\partial}{\partial y}(x\overline{\rho v})=0 \tag{6}$$

$$\rho u\frac{\partial u}{\partial x}+\overline{\rho v}\frac{\partial u}{\partial y}=\frac{\partial}{\partial y}\left(\mu\frac{\partial u}{\partial y}-\rho\overline{u'v'}\right) \tag{7}$$

$$\rho u\frac{\partial H}{\partial x}+\overline{\rho v}\frac{\partial H}{\partial y}=\frac{\partial}{\partial y}\left[\frac{\mu}{Pr}\frac{\partial H}{\partial y}+\mu\left(1-\frac{1}{Pr}\right)\frac{\partial}{\partial y}\left(\frac{u^2}{2}\right)-\rho\overline{v'H'}\right] \tag{8}$$

where $w_\theta=\partial w/\partial\theta$.

It is well known that for laminar flows with nonporous walls and wall temperatures independent of x, or adiabatic wall conditions, Eqs. (1-4) have similarity solutions if we define the similarity variable η by

$$d\eta = \left(\frac{u_e}{\rho_e\mu_e x}\right)^{1/2}\rho dy \tag{9}$$

In addition, if we introduce a two-component vector potential such that

$$\rho u x = \frac{\partial\psi}{\partial y}, \quad \rho w x = \frac{\partial\phi}{\partial y}, \quad \overline{\rho v}x = -\frac{\partial\psi}{\partial x} - \frac{1}{x}\frac{\partial\phi}{\partial\theta} \tag{10}$$

and dimensionless functions ψ and ϕ by

$$\psi = (\rho_e\mu_e u_e)^{1/2}x^{3/2}f(\theta,\eta), \quad \phi = (\rho_e\mu_e u_e)^{1/2}x^{3/2}\frac{w_e}{u_e}g(\theta,\eta) \tag{11}$$

then it can be shown that the two momentum equations, (2) and (3), and the energy equation (4) can be written as

$$(bf'')' + \frac{3}{2}ff'' + m_1 gf'' + m_2^2[(g')^2 - f'g'] = m_2\left(g'\frac{\partial f'}{\partial\theta} - f''\frac{\partial g}{\partial\theta}\right) \tag{12}$$

$$(bg'')' + \frac{3}{2}fg'' + m_1 gg'' + m_3\left[\frac{\rho_e}{\rho} - (g')^2\right] + \frac{\rho_e}{\rho} - f'g' = m_2\left(g'\frac{\partial g'}{\partial\theta} - g''\frac{\partial g}{\partial\theta}\right) \tag{13}$$

$$\left[\frac{C}{Pr}\left(1+\sqrt{2}\epsilon_m^+\frac{Pr}{Pr_t}\right)E' + \frac{Cu_e^2}{H_e}\left(1-\frac{1}{Pr}\right)(f'f'' + m_2^2 g'g'')\right]' + \frac{3}{2}fE' + m_1 gE' = m_2\left(g'\frac{\partial E}{\partial\theta} - E'\frac{\partial g}{\partial\theta}\right) \tag{14}$$

where primes denote differentiation with respect to η. Here we have used the eddy viscosity and turbulent Prandtl number concepts and have written the turbulence terms by[8]

$$-\rho\overline{u'v'} = \rho\epsilon_m\frac{\partial u}{\partial y}, \quad -\rho\overline{w'v'} = \rho\epsilon_m\frac{\partial w}{\partial y} \tag{15a}$$

$$-\rho\overline{v'H'} = \sqrt{2}\frac{\epsilon_m}{Pr_t}\frac{\partial H}{\partial y} \tag{15b}$$

The definitions of some of the terms in Eqs. (12-14) are:

$$f' = \frac{u}{u_e}, \quad g' = \frac{w}{w_e}, \quad E = \frac{H}{H_e}, \quad b = C(1+\epsilon_m^+)$$

$$\epsilon_m^+ = \frac{\epsilon_m}{\nu}, \quad C = \frac{\rho\mu}{\rho_e\mu_e}, \quad m_1 = m_3 - \frac{m_2^2}{2} + \frac{1}{2}\frac{m_2}{\rho_e\mu_e}\frac{d}{d\theta}(\rho_e\mu_e),$$

$$m_2 = \frac{w_e}{u_e}, \quad m_3 = \frac{1}{u_e}\frac{dw_e}{d\theta} \tag{16}$$

Similarly, Eqs. (5-8) can be transformed and expressed in a form similar to those given by Eqs. (12-14) by using the transformations given by Eqs. (9-11) with slight modification to the following parameters,

$$\rho w_\theta = \frac{\partial\phi}{\partial y}, \quad \overline{\rho v}x = -\frac{\partial\psi}{\partial x} - \phi \tag{17}$$

$$\psi = (\rho_e\mu_e u_e)^{1/2}x^{3/2}f(\eta), \quad \phi = (\rho_e\mu_e u_e x)^{1/2}\frac{(w_e)_\theta}{u_e}g(\eta) \tag{18}$$

Eqs. (5-8) then become

$$(bf'')' + \frac{3}{2}ff'' + m_3 gf'' = 0 \tag{19}$$

$$(bg'')' + \frac{3}{2}fg'' + m_3 gg'' + m_3\left[\frac{\rho_e}{\rho} - (g')^2\right] + \frac{\rho_e}{\rho} - f'g' = 0 \tag{20}$$

$$\left[\frac{C}{Pr}\left(1+\sqrt{2}\epsilon_m^+\frac{Pr}{Pr_t}\right)E' + \frac{Cu_e^2}{H_e}\left(1-\frac{1}{Pr}\right)ff''\right]' + \frac{3}{2}fE' + m_3 gE' = 0 \tag{21}$$

Here

$$f' = \frac{u}{u_e}, \quad g' = \frac{w_\theta}{(w_e)_\theta}$$

The usual procedure that has been followed in predicting the boundary-layer development on cones at incidence is to solve the system of equations given by Eqs. (14-21) for $\theta = 0$, and Eqs. (12-14) for $\theta > 0$ for both laminar and turbulent flows with a mixing-length or eddy-viscosity formulation with the following boundary conditions:

$$\eta = \circ \quad f = g = f' = g' = 0 \quad E'_w \text{ or } E_w \text{ given} \tag{22a}$$

$$\eta = \eta_\infty \quad f' = g' = E = 1 \tag{22b}$$

In those calculations it is assumed that the square-root variation of boundary-layer thickness for laminar flows also applies for turbulent flows.

Here, in this Note, we do not follow this procedure for turbulent flows; instead we follow a recent suggestion by Bradshaw et al.[7,9] and assume that the velocity profiles u/u_e and w/w_e are similar if we define $Y = y/x$, rather than $y/\sqrt{x}$. It follows then that for any quantity q

$$\left(\frac{\partial q}{\partial x}\right)_y = \left(\frac{\partial q}{\partial x}\right)_Y + \left(\frac{\partial q}{\partial Y}\right)_x\frac{\partial Y}{\partial x} \tag{23a}$$

$$\left(\frac{\partial q}{\partial y}\right)_x = \left(\frac{\partial q}{\partial Y}\right)_x\frac{\partial Y}{\partial y} \tag{23b}$$

To have similarity $(\partial q/\partial x)_Y = 0$; then noting that $\partial Y/\partial x = -y/x^2$ and $\partial Y/\partial y = 1/x$, from Eq. (23) we can write

$$\frac{(\partial q/\partial x)_y}{(\partial q/\partial y)_x} = \frac{(\partial q/\partial Y)_x(\partial Y/\partial x)}{(\partial q/\partial Y)_x(\partial Y/\partial y)} = -\frac{y}{x} \tag{24}$$

so that

$$\frac{\partial q}{\partial x} = -\frac{y}{x}\frac{\partial q}{\partial y} \tag{25}$$

With this assumption, it can be shown that Eqs. (1-4) can be written as

$$\frac{\partial}{\partial\theta}(\rho w) + \frac{\partial}{\partial y}(x\rho\hat{v}) + 2\rho u = 0 \tag{26}$$

$$\rho\frac{w}{x}\frac{\partial u}{\partial\theta} + \rho\hat{v}\frac{\partial u}{\partial y} - \rho\frac{w^2}{x} = \frac{\partial}{\partial y}\left(\mu\frac{\partial u}{\partial y} - \rho\overline{u'v'}\right) \tag{27}$$

$$\rho\frac{w}{x}\frac{\partial w}{\partial\theta}+\rho\hat{v}\frac{\partial w}{\partial y}+\rho\frac{uw}{x}=-\frac{1}{x}\frac{dp}{d\theta}+\frac{\partial}{\partial y}\left(\mu\frac{\partial w}{\partial y}-\rho\overline{w'v'}\right) \quad (28)$$

$$\rho\frac{w}{x}\frac{\partial H}{\partial\theta}+\rho\hat{v}\frac{\partial H}{\partial y}=\frac{\partial}{\partial y}\left[\frac{\mu}{Pr}\frac{\partial H}{\partial y}\right.$$
$$\left.+\mu\left(1-\frac{1}{Pr}\right)\frac{\partial}{\partial y}\left(\frac{u^2+w^2}{2}\right)-\rho\overline{v'H'}\right] \quad (29)$$

where

$$\hat{v}=\frac{\overline{\rho v}}{\rho}-u\frac{y}{x} \quad (30)$$

Similarly, the windward stagnation-line equations can be written as

$$\rho w_\theta+\frac{\partial}{\partial y}x\rho\hat{v}+2\rho u=0 \quad (31)$$

$$\rho\hat{v}\frac{\partial u}{\partial y}=\frac{\partial}{\partial y}\left(\mu\frac{\partial u}{\partial y}-\rho\overline{u'v'}\right) \quad (32)$$

$$\rho\hat{v}\frac{\partial w_\theta}{\partial y}+\rho\frac{w_\theta^2}{x}+\rho\frac{uw_\theta}{x}=-\frac{1}{x}\frac{d^2p}{d\theta^2}+\frac{\partial}{\partial y}\left[\mu\frac{\partial w_\theta}{\partial y}-\rho(\overline{w'v'})_\theta\right] \quad (33)$$

$$\rho\hat{v}\frac{\partial H}{\partial y}=\frac{\partial}{\partial y}\left[\frac{\mu}{Pr}\frac{\partial H}{\partial y}+\mu\left(1-\frac{1}{Pr}\right)\frac{\partial}{\partial y}\left(\frac{u^2}{2}\right)-\rho\overline{v'H'}\right] \quad (34)$$

If we now apply the transformation given by Eqs. (9-11) with $\rho\hat{v}x$ defined by

$$\rho\hat{v}x=-2\frac{\psi}{x}-\frac{1}{x}\frac{\partial\phi}{\partial\theta} \quad (35)$$

to Eqs. (26-29) and the transformation given by Eqs. (17) and (18) with $\rho\hat{v}x$ defined by

$$\rho\hat{v}x=-2\frac{\psi}{x}-\frac{\phi}{x} \quad (36)$$

to Eqs. (31-34), it can be shown that the resulting transformed equations are almost identical to those given by Eqs. (12-14) for the general case and to those given by Eqs. (19-21) for the windward stagnation line case. The only difference appears in the coefficients of ff'', fg'' and fE'; instead of 3/2, the new equations have a coefficient of 2. It should be noted, however, that the resulting equations for turbulent flows are not strictly similar like the laminar flow equations because they were derived under the assumption of constant x. Thus the equations are valid for a fixed x and no scaling of solutions is allowed.

Comparison with Experiment

We have used the numerical method of Ref. 10 and the eddy-viscosity formulation of Refs. 2, 3, and 4 (see also Ref. 8) to obtain a solution of the system of equations given by Eqs. (19-21 and 12-14) subject to Eq. (22). Figure 1 shows a comparison of calculated and experimental results for the data of Rainbird,[11] which is for a 12.5-degree half-angle cone at an angle of attack of 15.78 degrees in supersonic stream with freestream Mach number 1.8. The Reynolds number of the cone, based on its axial length, was 25×10^6, which indicates that the possible effect of flow nonuniformities caused by variable transition location upon the measurements at $0.85L$ can be neglected.

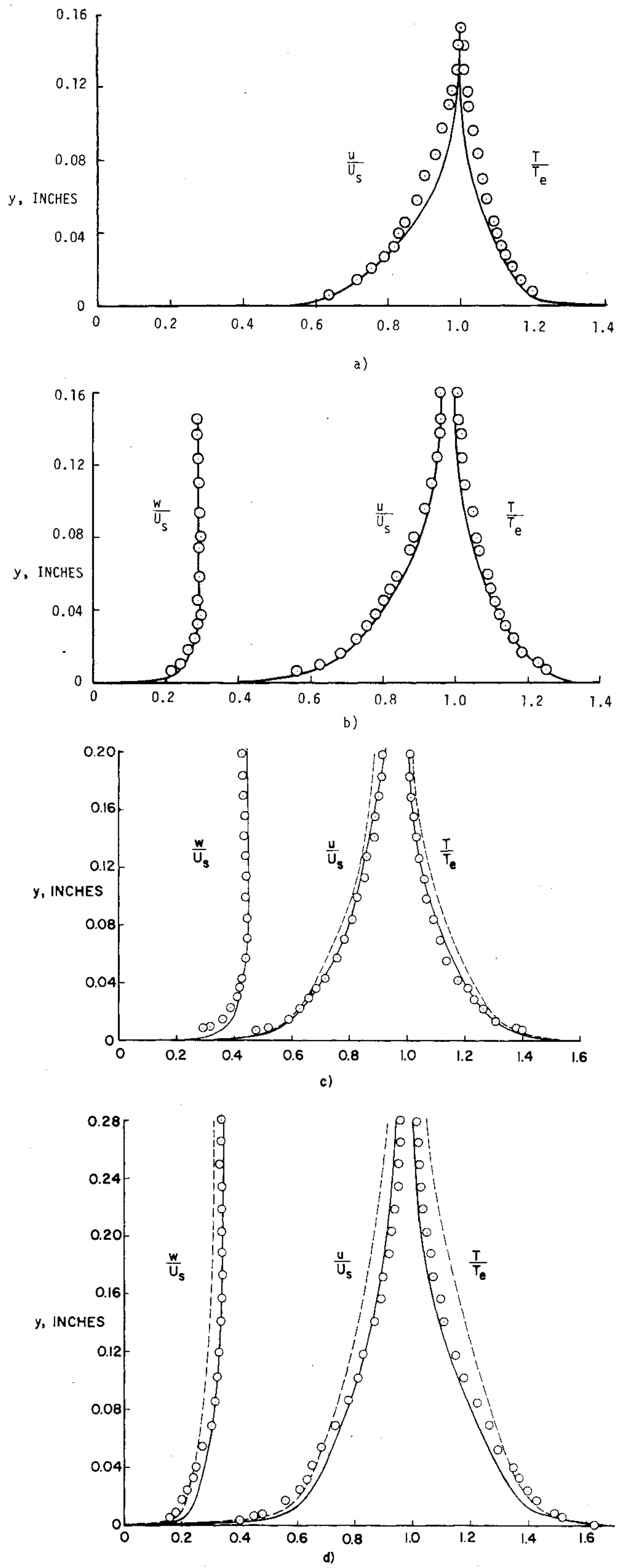

Fig. 1 Comparison of measured and calculated turbulent velocity and temperature profiles for the data of Rainbird.[11] Data at 0.85 x/L from the cone tip for: a) $\phi=0°$; b) $\phi=45°$; c) $\phi=90°$; and d) $\phi=135°$. Dashed lines denote calculations where the "old" procedure differs from the present one.

The computed results shown in Fig. 1 were made by using both the "old" and the "new" procedures. According to the comparison of results with experiment, we observe that the results obtained with the new procedure give better agreement with experiment than the old procedure. For circumferential angles $\phi = 0$ and 45° (Figs. 1a, 1b), however, there is very little difference between the computed results obtained by either procedure; as ϕ increases, so does the difference as shown in Figs. 1c and 1d.

A note should be made of the discrepancies in the temperature and velocity profiles at $\phi = 135°$. Because of the relatively high angle of attack, the flow beyond about $\phi = 120°$ is subject to adverse pressure gradient, which eventually leads to separation defined by zero shear stress component normal to the generator. Although our calculations with either procedure predict separation at about $\phi = 161°$, close to the measured value of $\phi = 159°$, the measured boundary layer shows a more rapid thickening than is predicted by calculations. This can be traced to vortex formation, in which case the ordinary boundary-layer equations are no longer valid anyway.

In summary we conclude that the similarity variable proposed by Bradshaw for turbulent flows over tapered wings is also applicable to the calculation of high Reynolds number turbulent boundary layer on cones at incidence with local similarity assumptions.

Although the improvements obtained by the "new" procedure may seem small in comparison with the empiricism contained in eddy-viscosity laws and viscous/inviscid interaction effects, they are nevertheless encouraging that the local similarity will work for other similar shapes as well. In principle, the procedure is strictly applicable to conical bodies with arbitrary cross-section provided that the radial pressure gradient is very small.

The computer time (CPU) for the present case with 1894 net points in the cross-flow plane was 7.86 sec (0.0042 sec/net point) on an IBM 370/165 computer.

Acknowledgment

This work was supported by Naval Air Systems Command under Contract N60921-76-C-0089.

References

[1] Cebeci, T. and Smith, A. M. O., *Analysis of Turbulent Boundary Layers*, Academic Press, New York, 1974.

[2] Cebeci, T., "Calculation of Three-Dimensional Boundary Layers, I. Swept Infinite Cylinders and Small Cross Flow," *AIAA Journal*, Vol. 12, June 1974, pp. 779-786.

[3] Cebeci, T., Calculation of Three-Dimensional Boundary Layers, II. Three-Dimensional Flows in Cartesian Coordinates," *AIAA Journal*, Vol. 13, Aug. 1975, pp. 1056-1064.

[4] Cebeci, T. and Abbott, D. E., "Boundary Layers on Rotating Disk," *AIAA Journal*, Vol. 13, June 1975, pp. 829-832.

[5] Adams, J. C., Jr., "Three-Dimensional Compressible Turbulent Boundary Layers on a Sharp Cone Incidence in Supersonic Flow," *International Journal of Heat and Mass Transfer*, Vol. 17, May 1974, pp. 581-595.

[6] Bontoux, P. and Roux, B., "Compressible Turbulent Boundary Layer on a Yawed Cone," *AIAA Journal*, Vol. 14, May 1976, pp. 545-546.

[7] Bradshaw, P., Mizner, C. A., and Unsworth, K., "Calculations of Compressible Turbulent Boundary Layers on Straight-Tapered Swept Wings," *AIAA Journal*, Vol. 14, March 1976, pp. 399-400.

[8] Cebeci, T., Kaups, K., and Rehn, J. A., "Some Problems of the Calculation of Three-Dimensional Boundary-Layer Flows on General Configurations," NASA CR-2285, July 1973.

[9] Bradshaw, P., Mizner, G. A., and Unsworth, K., "Calculation of Compressible Turbulent Boundary Layers with Heat Transfer on Straight-Tapered Swept Wings," Imperical College Aero Rept. 75-04, May 1975.

[10] Keller, H. B. and Cebeci, T., "Accurate Numerical Methods for Boundary Layers. II. Two-Dimensional Turbulent Flows," *AIAA Journal*, Vol. 10, Sept. 1972, pp. 1197-1200.

[11] Rainbird, W. J., "Turbulent Boundary-Layer Growth and Separation on a Yawed Cone," *AIAA Journal*, Dec. 1968, pp. 2140-2146.

Analytical and Experimental Study of Turbulent Methane-Fired Backmixed Combustion

R. E. Peck* and G. S. Samuelsen†
UCI Combustion Laboratory, University of California, Irvine, Calif.

Nomenclature

D = combustor diameter
K = constant in effective viscosity expression
L = length of flowfield
r = radius
T = temperature
V = velocity
μ = viscosity
ρ = density
ϕ = equivalence ratio, $\dfrac{(F/A)\ \text{actual}}{(F/A)\ \text{stoichiometric}}$

I. Introduction

THE present results are from a continuing investigation designed to improve the prediction of reacting, recirculating flows and to clarify the mechanisms of pollutant formation in continuous combustion systems. The combustor configuration is a 51mm diameter axisymmetric duct containing an aerodynamic (opposed-jet) flameholder as shown in Fig. 1. The opposing, high-velocity jet stream serves to stabilize the flame by backmixing hot combustion products with fresh reactants (premixed methane/air).

The analytical model of the opposed-jet combustor (OJC) flowfield is founded on extended versions of the PISTEP method of Gosman et al.[1] The numerical procedure solves simultaneously the governing elliptic partial differential conservation equations with the corresponding dependent variables as follows: conservation of mass—stream function, ψ; conservation of momentum—vorticity, ω/r; conservation of energy—enthalpy, $\bar{h}$; species continuity—mass fraction, m_j. A simplified effective viscosity model for turbulent momentum transport is adopted for the present investigation[1]:

$$\mu_{\text{eff}} = KD^{2/3} L^{1/3} \rho^{2/3} (\dot{m} V^2)^{1/3} \tag{1}$$

Exchange coefficients for turbulent energy and mass transport are related to μ_{eff} by effective Prandtl and Schmidt numbers. The OJC geometry was initially incorporated into the computational procedure by Samuelsen and Starkman for an ammonia/air fired system.[2] A numerical solution for the methane/air system including the formation of the pollutant species CO and NO was later incorporated.[3] The present study compares the numerical prediction of local flowfield properties for the methane/air system with experimentally determined values.

II. Approach

Cold Flow

Consideration of cold flow conditions enables a preliminary evaluation of the transport models incorporated into the numerical procedure. The cold flow solution is ob-

Received July 15, 1976; revision received Jan. 17, 1977.

Index categories: Reactive Flows; Combustion in Gases; Air-breathing Propulsion, Subsonic and Supersonic.

*Research Assistant; present address Department of Mechanical Engineering, University of Kentucky, Lexington, Ky.

†Associate Professor, Mechanical and Environmental Engineering.